THE JOURNAL OF BIOLOGICAL CHEMISTRY VOL. 284, NO. 25, pp. 17340–17351, June 19, 2009

Autoprocessing of the *Escherichia coli* AIDA-I Autotransporter

*A NEW MECHANISM INVOLVING ACIDIC RESIDUES IN THE JUNCTION REGION**

Received for publication, March 18, 2009, and in revised form, April 17, 2009 Published, JBC Papers in Press, April 27, 2009, DOI 10.1074/jbc.M109.010108

Marie-Ève Charbonneau, Julie Janvore[1], and Michael Mourez[2]

From the Canada Research Chair on Bacterial Animal Diseases, Université de Montréal, Faculté de Médecine Vétérinaire, 3200 Sicotte, St.-Hyacinthe, Québec J2S 7C6, Canada

The cleavage of the autotransporter adhesin involved in diffuse adherence (AIDA-I) of *Escherichia coli* yields a membrane-embedded fragment, AIDAc, and an extracellular fragment, the mature AIDA-I adhesin. The latter remains noncovalently associated with AIDAc but can be released by heat treatment. In this study we determined the mechanism of AIDA-I cleavage. We showed that AIDA-I processing is an autocatalytic event by monitoring the *in vitro* cleavage of an uncleaved mutant protein isolated from inclusion bodies. Furthermore, by following changes in circular dichroism spectra and protease resistance of the renaturated protein, we showed that the cleavage of the protein is correlated with folding. With site-directed deletions, we showed that the catalytic activity of the protein lies in a region encompassing amino acids between Ala-667 and Thr-953, which includes the conserved junction domain of some autotransporters. With site-directed point mutations, we also found that Asp-878 and Glu-897 are involved in the processing of AIDA-I and that a mutation preserving the acidic side chain of Asp-878 was tolerated, giving evidence that this carboxylic acid group is directly involved in catalysis. Last, we confirmed that cleavage of AIDA-I is intramolecular. Our results unveil a new mechanism of auto-processing in the autotransporter family.

Monomeric autotransporters, secreted by the type Va secretion pathway, constitute one of the largest family of secreted proteins in Gram-negative bacteria (1). Various virulence attributes have been associated with most autotransporters, such as adhesion or invasion, self-association, biofilm formation, serum resistance, and cytotoxic activity to name just a few (2, 3). Autotransporters are synthesized as pre-proproteins with modular organizations. An N-terminal *sec*-dependent signal sequence permits the secretion of the protein across the inner membrane (4). A C-terminal membrane-embedded domain promotes secretion of parts of the protein across the outer membrane and is composed of a β-barrel and a α-helix spanning its lumen (5, 6). The central domain of the protein is, thus, extracellular and bears its functional part. In some cases the extracellular part of the protein is cleaved and remains associated with the outer membrane or is secreted in the extracellular milieu. Directly preceding the membrane-embedded domain, a functional subdomain of ~100 amino acids is sometimes present in the extracellular domain and has been called the junction region (also named autochaperone domain or stable core) (7–9). This region is essential for stabilizing the β-barrel and/or to promote folding of the extracellular domain (7–9).

The adhesin involved in diffuse adherence (AIDA-I)[3] is a monomeric autotransporter that has been extensively studied. AIDA-I was originally identified as a plasmid-encoded protein from a diffusely adhering *Escherichia coli* strain isolated in a case of infantile diarrhea (10). This adhesin was then shown to play a role in neonatal and postweaning diarrheal diseases in piglets, both of which cause major economic losses in farms worldwide (11–13). Besides its role as an adhesin, AIDA-I has been shown to mediate self-association and biofilm formation (14) as well as invasion of epithelial cells (15). Additionally, this protein undergoes a modification that is rare in bacteria, as it is *O*-glycosylated by the specific cytoplasmic protein autotransporter adhesin heptosyltransferase (Aah) (16, 17). AIDA-I has been suggested to be a member of a new group of autotransporter called self-associating autotransporters, which includes the Ag43 aggregation factor and the TibA invasin (18).

After secretion at the cell surface, the extracellular domain of the protein, called mature AIDA-I, is cleaved from the C-terminal domain, called AIDAc, which encompasses the β-barrel, the α-helix, and the junction region (19, 20). Mature AIDA-I, however, remains strongly associated with AIDAc (15). The processing of AIDA-I is neither essential for the multiple functions of the protein nor for its stability (15). Questions remain about the mechanism involved in this cleavage. In a few autotransporters, the cleavage reaction involves an exogenous protease. IcsA for instance, an autotransporter of *Shigella flexneri*, is cleaved by a dedicated outer membrane protease called IcsP, which is related to the OmpT protease found in *E. coli* (21). Similarly, the *Neisseria meningitidis* serine protease NalP is specifically responsible for the partial processing of various autotransporters, including the IgA protease (22), App (22), AusI (23), and MspA (24). In contrast, the cleavage of AIDA-I is not mediated by the known *E. coli* periplasmic or outer membrane proteases (DegP, OmpT, or OmpP), and it occurs in

* This work was supported by financial contributions from the Groupe de Recherche et d'Études sur les Maladies Infectieuses du Porc (GREMIP), Canadian Institutes of Health Research Grant 84578, Canada Research Chair program and the Canada Foundation for Innovation Grant 201414, and a graduate fellowship from the Natural Sciences and Engineering Research Council of Canada (Grant 85297596, to M.-È. C.).

[1] Present address: Institut Curie, UMR144; 26 rue d'Ulm; 75248 Paris Cedex 05, France.

[2] To whom correspondence should be addressed. Tel.: 450-773-8521 (ext. 18430); Fax: 450 778 8108; E-mail: m.mourez@umontreal.ca.

[3] The abbreviations used are: AIDA-I, adhesin involved in diffuse adherence; Aah, autotransporter adhesin heptosyltransferase; IPTG, isopropyl-β-thiogalactopyranoside; SPATE, serine protease autotransporters of *Enterobacteriaceae*; TBS, Tris-buffered saline; Tricine, *N*-[2-hydroxy-1,1-bis(hydroxymethyl)ethyl]glycine; WT, wild type.

E. coli as well as in *Shigella* or *Salmonella* strains (19). Based on those observations, this processing has been suggested to be an autocatalytic event, even though no protease catalytic site can be identified in the protein.

Two types of autocatalytic processing mechanisms have been described in other autotransporters. The Hap autotransporter of *Haemophilus influenzae* (25), the SphB1 protein of *Bordetella pertussis* (26), and the NalP (22), App (27), and IgA proteases of *N. meningitidis* (28) cleave themselves by an endogenous serine protease domain. More recently, it was shown that the serine protease autotransporters of *Enterobacteriaceae* (SPATE) family cleave themselves in the α-helix located in the lumen of the membrane-embedded β-barrel by a catalytic reaction that involves an aspartate and a conserved asparagine (6, 29). The same autocatalytic reaction has been shown for two distantly related *B. pertussis* autotransporters, pertactin and BrkA (29). However, none of these mechanisms can be hypothesized for AIDA-I cleavage; AIDA-I possesses neither a serine protease domain like Hap nor the asparagine residue required for the SPATE cleavage. In addition, the AIDA-I cleavage site is not located in the α-helix. Thus, the mechanism of AIDA-I processing must be different and remains unknown.

The mechanisms by which a diversity of other autotransporters are cleaved remain unknown. This is for instance the case for the *E. coli* Ag43 self-associating autotransporters (30), the *Helicobacter pylori* VacA cytotoxin (31), the *Chlamydia pneumoniae* polymorphic membrane proteins (32), and the Ssp proteins of *Serratia marcescens* (33) as well as the cohemolysin Cfa (34) and the Arp immunogenic protein of *Bartonella henselae* (35).

In this study we determined the mechanism of AIDA-I cleavage. We first showed that a truncated mutant of AIDA-I can refold *in vitro* and undergo self-cleavage, providing definite proof for the autocatalytic mechanism. By constructing site-directed deletions and point mutations, we then showed that the catalytic domain lies in the region encompassing the amino acids between Ala-667 and Thr-953, and we identified two residues in the junction region, Asp-878 and Glu-897, that are essential for processing. Last, we confirmed that the mechanism of proteolysis for AIDA-I is intramolecular. This is the first report of this type of autocatalytic activity.

EXPERIMENTAL PROCEDURES

Bacterial Strains and Plasmids—The *E. coli* K12 strains C600 (obtained from New England Biolabs, genotype: F^-, *thr*1, *leuB*6, *thi*1, *lacY*1, *supE*44, *rfbD*1, *fhuA*21) and BL21 (obtained from Stratagene, genotype: F^-, *ompT*, *hsdS*($r_B^-m_B^-$), *gal*) were used in this study. Plasmid pAgH has been described before and allows expression of Aah and of AIDA-I tagged at the N terminus of the proprotein with six histidine amino acids and a glycine (His tag) (15). All point mutations in the pAgH plasmids were introduced by oligonucleotide-directed mutagenesis with the QuikChange II site-directed mutagenesis kit (Stratagene) using the primers listed in Table 1 and their corresponding complementary oligonucleotides. The pAngH (allowing expression of AIDA-I without Aah), pAngHΔSS (deletion of amino acids 1–49), pAngHΔN (deletion of amino acids 54 to 225), and pAngHΔC2 (deletion of amino acids 224–667) plasmids were described elsewhere (36, 37). The Δ$\alpha\beta$ deletion (deletion of amino acids 953–1286) was introduced into pAngHΔSS also by site-directed mutagenesis using primers listed in Table 1, generating the pAngHΔSSΔ$\alpha\beta$ plasmid. For glycosylation, we used plasmid pAah, a derivative of pACYC-184 described elsewhere (17). Plasmid pACYC-AgH was obtained by subcloning in the pAah vector the DNA fragments from pAgH generated by restriction enzymes XbaI and BrsGI.

TABLE 1
Primers used in this study

Primer	Sequence
SSΔ$\alpha\beta$	5′-GGTATTTAACCAGTTAACTTCCCACATCTGATACCCGG-3′
D712A	5′-GGACTAACATTCAGAACGCCGGCAATTTCATTCTCAATCTTGC-3′
D724A	5′-GCTGAAAACTATGCTTTTGAAACAGAGCTCTCAGGTAGTGG-3′
D772A	5′-GCAGTAGTCAATGCAGCCATGGCTGTCAACCAGAATGCC-3′
D785A	5′-GCCTATATAAACATTAGTGCACAGGCAACAATTAATGG-3′
E845A	5′CTTAATCCTACAAAAGCTAGCGCAGGTAATACTCTTACCG-3′
N849A	5′CCTACAAAAGAAAGTGCCGGCGCTACTCTTACCGTGTC-3′
E871A	5′CTCTTGGTGGTGTGCTTGCCGGCGATAATTCACTTACGG-3′
D873A	5′-CTCTTGGTGGTGTTCTAGAAGGAGCTAATTCACTTACGG-3′
N874A	5′-GCTTGAAGGAGATGCTAGCCTTACGGACCGTCTGGTGG-3′
D878A	5′-GGAGATAATTCACTTACGGCCCGACTAGTGGTGAAAGGTAATACC-3′
D878E	5′-GGAGATAATTCACTTACGGAACGACTAGTGGTGAAAGGTAATACC-3′
D878N	5′-GGAGATAATTCACTTACGAACCGGTTGGTGGTGAAAGGTAATACC-3′
R879A	5′-GGAGATAATTCACTTACGGACGCACTAGTGGTGAAAGGTAATACC-3′
E897A	5′-GGTCAAAGTGACATCGTTTATGTTAACGCAGATGGCAGTGGTGG-3′
E897Q	5′-GGTCAAAGTGACATCGTTTATGTTAACCAAGATGGCAGTGGTGG-3′
D906A	5′-GGTGGTCAGACTCGAGCTGGTATTAATATTATTTCTGTAGAGGG-3′
D933A	5′-CGCGTAGTTGCCGGAGCATATGCTTACACACTGCAGAAAGG-3′
D1021A	5′-GGTAAGCTTAATGCCGGCCAAAATAAAACAACAACC-3′
D1117A	5′-GCATCAGTGAAAGGTGCCGGCCTGGAAGAAG-3′
D1170-5A	5′-GGGGTTACGCCGGCTACACATCAGGAGGCTAACGGAACG-3′
D1078A	5′-GCTGCCAGAAACACGCTAGCTGGTTATTCTGTCGGGG-3′
D1233-4A	5′-GGTGTTAAAATGAGTGCTGCTAGCCAGTTGTTGTCAGG-3′

Functional Assays—The functionality of the uncleaved mutant pAgHD878N was determined by the functional assays for adhesion, autoaggregation, and biofilm formation, as previously described (15).

Bacteria Growth and Induction Conditions—Bacteria containing the different plasmids were grown on Luria-Bertani (LB) agar plates or in LB broth containing 100 $\mu g \cdot ml^{-1}$ ampicillin and, when required, 50 $\mu g \cdot ml^{-1}$ chloramphenicol. Bacterial cultures were grown at 30 °C and induced with 10 μM isopropyl-β-thiogalactopyranoside (IPTG) when they reached an optical density at 600 nm ($A_{600\ nm}$) of 0.8, unless indicated otherwise. This low concentration of IPTG was used to limit the toxicity associated with overexpression of AIDA-I. To produce inclusion bodies, bacteria were grown at 37 °C until an $A_{600\ nm}$ of 0.8 and induced overnight with 1 mM IPTG.

SDS-PAGE and Immunoblotting—Protein samples were diluted in twice-concentrated SDS-PAGE loading buffer containing β-mercaptoethanol and denatured by heating at 100 °C for 10 min. The samples were then separated by SDS-PAGE on 10% acrylamide gels. The gels were either stained with Coomassie Blue or transferred to polyvinylidene fluoride membranes (Millipore). Immunodetection was performed with anti-His antibodies (Applied Biological Materials) diluted 1:10,000 in blocking buffer (5% skim milk, 50 mM Tris-HCl, pH 7.5, 150 mM NaCl, 0.05% Triton X-100). A rabbit anti-mouse horseradish peroxidase-conjugated antibody (Sigma) was used as a secondary antibody according to the instructions of the manufacturer. Immune complexes were revealed using a 3,3′,5,5′-tetramethylbenzidine solution for membranes (Sigma).

Whole-cell Extracts—Overnight cultures were grown, normalized, and centrifuged for 15 min at 12,000 × *g* in microcen-

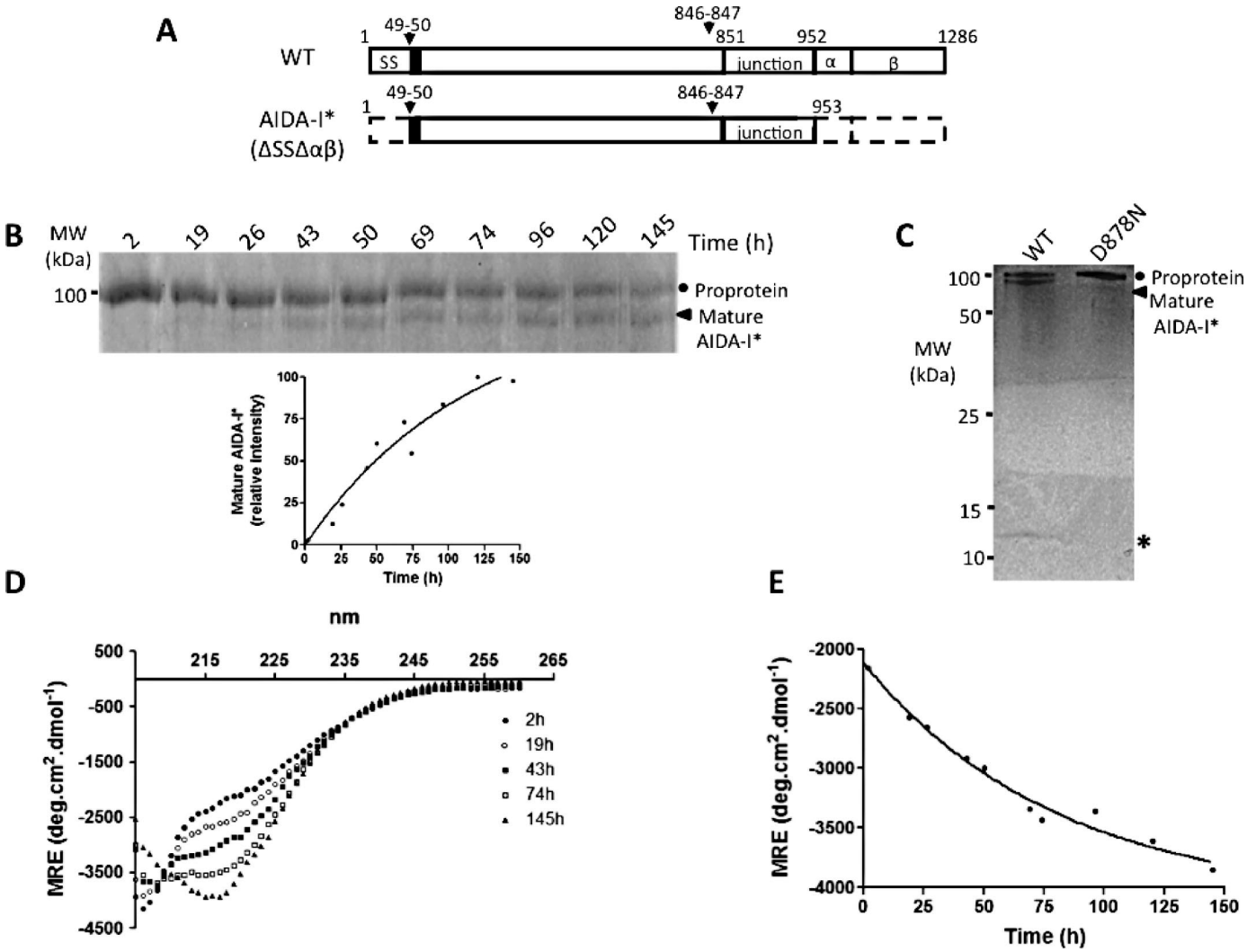

FIGURE 1. **Cleavage of AIDA-I* *in vitro*.** *A*, schematic diagram of the AIDA-I* construct, showing plasmid pAngH (*WT*) and pAngHΔSSΔ$\alpha\beta$ (Δ*SS*Δ$\alpha\beta$ or *AIDA-I**). The *filled box* represents the His tag at the N terminus of mature AIDA-I. *B*, inclusion bodies containing the AIDA-I* protein were collected, solubilized in 0.1 M Tris-HCl, pH 8, 6 M guanidinium hydrochloride, and purified by immobilized metal affinity chromatography. Renaturation of the AIDA-I protein was performed by first exchanging the buffer on a 1-ml His trap HP column for 2 h with renaturation buffer (TBS, pH 8, 0.1% Triton X-100). The protein was then eluted and left at 4 °C. At different times after buffer exchange, aliquots were taken and boiled in SDS-PAGE loading buffer. The proteins were then resolved by SDS-PAGE and the gel-stained with Coomassie Blue. The uncleaved (proprotein, *circles*) and cleaved (mature AIDA-I*, *arrowheads*) forms of the protein are indicated. The intensities of the bands were quantified and normalized to the maximal intensity. *C*, the WT and the uncleaved (D878N*) proteins 145 h after buffer exchange were separated by SDS-PAGE on a 16% Tris-Tricine gel. The *star* indicates the C-terminal cleaved peptide. *D*, far-UV CD spectra of the AIDA-I* protein at different times after buffer exchange. The ellipticities were recorded between 205 and 260 nm. *E*, the ellipticities at 218 nm were recorded at different times after the initial renaturation. *MRE*, mean residual ellipticity.

trifuge tubes, and the pellets were resuspended in 100 μl of phosphate-buffered saline. All samples were processed by SDS-PAGE and immunoblotting, as described above.

Analysis of the Intra- or Intermolecular Nature of AIDA-I Processing—Overnight cultures of *E. coli* C600 harboring plasmid pTRC99a, pAgH, or pAgHD878N were normalized at the same $A_{600\,nm}$ and co-incubated for 30 min at 30 °C. The samples were pelleted, and whole-cell extracts were obtained as described above. Alternatively, whole-cell extracts of overnight cultures *E. coli* C600 harboring plasmids pTRC99a/pACYC184, pACYC-AgH, pAgHD878N, or pACYC-AgH and pAgHD878N simultaneously were prepared as described above. For the *in vitro* experiment, native AIDA-I proteins (wild type and D878N mutant) were purified as described below. Pure proteins were incubated separately or together for 30 min at room temperature or for 2 h at 4 °C and resolved by SDS-PAGE, and the gels were stained with Coomassie Blue.

Purification of Native AIDA-I—The purification was performed as described previously (15). Briefly, 1 liter of overnight cultures of C600 harboring plasmids pAgH or pAgHD878N were grown until an $A_{600\,nm}$ of 0.8 and induced with 10 μM IPTG. Bacteria were harvested and resuspended in 50 ml of Tris-buffered saline (TBS: 50 mM Tris-HCl, pH 8, 150 mM NaCl) containing lysozyme (0.4 mg·ml^{-1} final concentration) and EDTA, pH 8 (10 mM final concentration), and lysed with a French press and an ultrasonic processor. Cellular debris was removed by low speed centrifugation. The lysate was centrifuged for 1 h in an ultracentrifuge at 250,000 × *g*. The membranes were resuspended in TBS containing 1% Triton X-100,

incubated for 1 h at room temperature, and centrifuged again. The solubilized membranes contained the histidine-tagged native AIDA-I. The proteins were purified using an ÄKTA purifier system with a 1-ml His Trap HP column (Amersham Biosciences) according to the instructions of the manufacturer. The purity of the purified proteins was confirmed by SDS-PAGE and staining with Coomassie Blue.

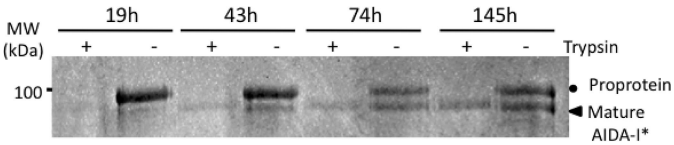

FIGURE 2. **Protease sensitivity of AIDA-I* during refolding.** Limited proteolysis of pure AIDA-I* was conducted for 30 min with 37 $\mu g \cdot ml^{-1}$ (final concentration) of trypsin at different times after buffer exchange. The proteins were resolved by SDS-PAGE and the gel stained with Coomassie Blue.

Purification of Inclusion Bodies and Refolding—One liter of *E. coli* BL21 harboring plasmid pAngHΔSSΔ$\alpha\beta$ or pAngHΔSSΔ$\alpha\beta$D878N and plasmid pAah were grown at 37 °C until an $A_{600\ nm}$ of 0.8 and induced overnight with 1 mM IPTG to allow formation of inclusion bodies. Bacteria were harvested and resuspended in 50 ml of TBS containing a proteases inhibitor mixture (Complete EDTA-free, Roche Applied Science) and lysed with a French press and an ultrasonic processor. Cellular debris was removed by low speed centrifugation. Inclusion bodies were collected by centrifugation at 4000 × *g* for 75 min. The pellets were resuspended in 30 ml of denaturing buffer (0.1 M Tris-HCl, pH 8, 6 M guanidinium hydrochloride) and centrifuged again at 16,000 × *g* for 1 h to remove any debris. Denatured proteins were purified using an ÄKTA purifier system with a 1-ml His Trap HP column as above.

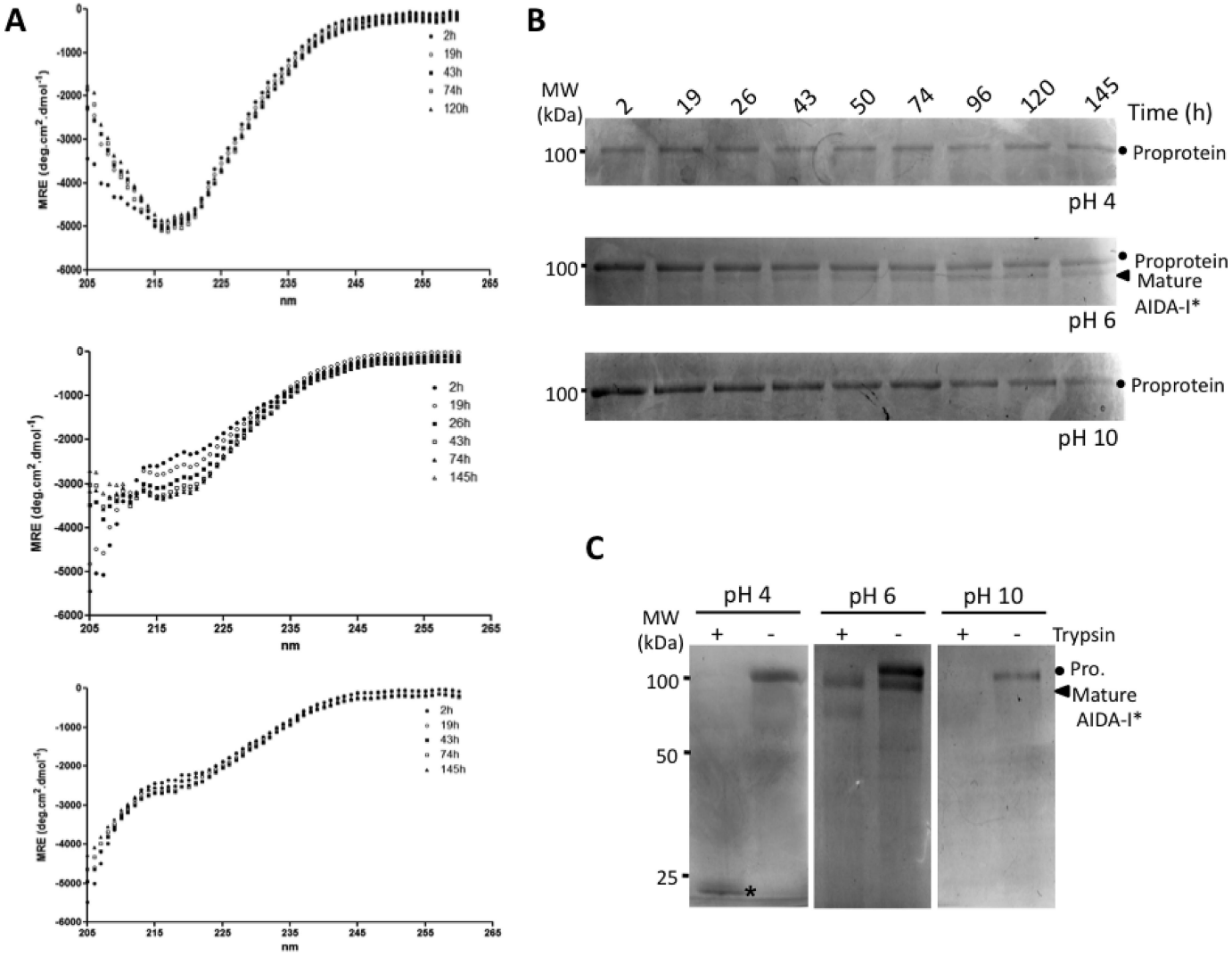

FIGURE 3. **Effect of pH on the *in vitro* folding of AIDA-I*.** Renaturation of the AIDA-I* protein was performed by first exchanging the buffer on a 1-ml His trap HP column for 2 h with renaturation buffer at pH 8. After elution, an equal amount of protein was diluted in buffer with different pH values (50 mM sodium citrate, pH 4 or 6; 50 mM Tris, pH 8; 50 mM sodium carbonate, pH 10, all supplemented with 150 mM NaCl and 0.1% Triton X-100) and left at 4 °C. *A*, far-UV CD spectra of the AIDA-I* protein at different times after buffer exchange for pH4 (*top*) pH 6 (*middle*) or pH 10 (*bottom*). The ellipticities were recorded between 205 and 260 nm. *MRE*, mean residual ellipticity. *B*, at different times after the buffer exchange aliquots were taken and boiled in SDS-PAGE loading buffer. *C*, limited proteolysis at 145 h after buffer exchange was performed as described in Fig. 2. For pH 4, the proteolysis was performed after a pH shift at pH 8. The proteins were resolved by SDS-PAGE and the gel-stained with Coomassie Blue. The uncleaved (proprotein, *circles*) and cleaved (mature AIDA-I*, *arrowheads*) forms of the protein are indicated.

Renaturation of the proteins was performed by a progressive replacement of the denaturing buffer with the renaturation buffer (TBS, pH 8, 0.1% Triton X-100, 100 μM phenylmethanesulfonyl fluoride, and Complete EDTA-free proteases inhibitor mixture) on a 1-ml His trap HP column for 2 h. The proteins were then eluted, and the imidazole was immediately eliminated using a PD-10 desalting column (Amersham Biosciences). The proteins were then kept at 4 °C for renaturation to proceed.

To study the effect of pH on the *in vitro* folding of AIDA-I, the initial renaturation was performed as above, except that the buffer contained 2 mM Tris-HCl, pH 8, rather than 50 mM Tris-HCl, pH 8. An equal amount of protein was diluted to a final concentration of 250 $\mu g \cdot ml^{-1}$ in buffers with different pH values (50 mM sodium citrate, pH4 and pH 6; 50 mM Tris-HCl, pH 8; 50 mM sodium carbonate, pH 10, all supplemented with 150 mM NaCl, 0.1% Triton X-100, 100 μM phenylmethanesulfonyl fluoride, and Complete EDTA-free) and left at 4 °C. 1 M Tris-Base was used to shift the pH from pH 4 to pH 8.

For the mass spectrometry experiment, the proteins (native or refolded *in vitro*) were reduced before in-gel digestion with trypsin. Tryptic peptides were separated with a SB-C18 ZORBAX 300 reverse-phase column, and mass spectra were recorded on a hybrid linear ion trap-triple quadripole mass spectrometer (Q-Trap; AB Applied Biosystems) equipped with a nanoelectrospray ionization source (F. Lépine, IAF-INRS, Laval, Canada).

Limited Proteolytic Digestion—Pure native proteins (wild type or D878N mutant) were incubated on ice for 30 min in the presence of different concentrations of trypsin, varying between 167 and 1 $\mu g \cdot ml^{-1}$ (final concentration). Alternatively, the renatured proteins were incubated on ice for 30 min in the presence or absence of trypsin at a final concentration of 37 $\mu g \cdot ml^{-1}$. Proteolysis was stopped by boiling samples for 10 min in SDS-PAGE loading buffer. All samples were processed by SDS-PAGE and Coomassie Blue staining as described above.

Far-UV Circular Dichroism (CD) Spectroscopy—Far-UV CD spectra were recorded in a 0.1-cm-path length cuvette between 205 and 260 nm using a spectropolarimeter (model J-810; Jasco spectroscopic Co. Ltd.). For each spectrum, 15 accumulations were averaged. Thermal denaturation was followed by monitoring the ellipticity at 218 nm with the temperature varying between 25 and 80 °C at a rate of 5 °C per min. Proteins concentration for all CD experiments was 190 $\mu g \cdot ml^{-1}$ in TBS containing 0.1% Triton X-100. Ellipticities were converted to mean residual ellipticities.

Structure Prediction and Alignment—The three-dimensional structural model of the junction region and the cleavage site of AIDA-I (amino acids Ile-807—Leu-956) were constructed using the Phyre program (38) and is based on the known crystal structure of *B. pertussis* pertactin (39). The schematic representation was generated using the PyMol software (Delano Scientific LLC). Sequence alignment was performed using the BLOSUM 62 matrix, with the Geneious Pro 4.0.2 software (Biomatters Ltd.).

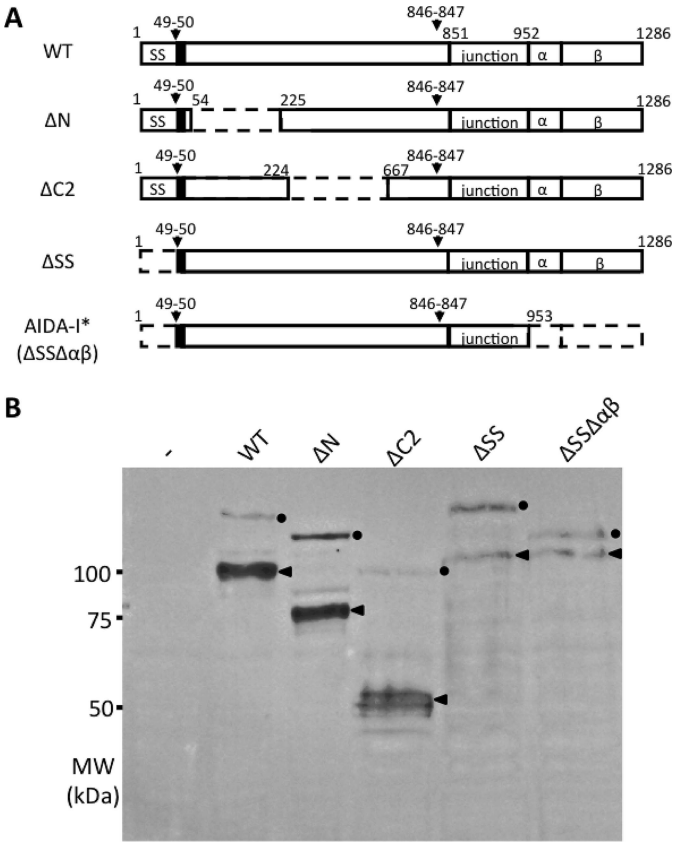

FIGURE 4. **Mapping of the region involved in AIDA-I cleavage.** *A*, schematic diagram of the deletion constructs showing plasmid pAngH (*WT*), pAngHΔN (Δ*N*), pAngHΔC2 (Δ*C2*), pAngHΔSS (Δ*SS*), and pAngHΔSSΔ$\alpha\beta$ (Δ*SS*Δ$\alpha\beta$ or *AIDA-I**). The *filled box* represents the His tag at the N terminus of mature AIDA-I. *B*, whole-cell lysates were obtained from overnight cultures of C600 harboring an empty vector (−), expressing wild-type AIDA-I (*WT*), or expressing the ΔN, ΔC2, ΔSS or ΔSSΔ$\alpha\beta$ mutants were obtained and probed with anti-His antibodies, which allowed detection of the proprotein (*circles*) and mature AIDA-I (*arrowheads*). All plasmids were transformed in bacteria expressing the Aah glycosyltransferase.

RESULTS

A Purified Mutant of AIDA-I Undergoes Self-cleavage in Vitro—As AIDA-I cleavage is thought to be autocatalytic, we decided to purify the unfolded glycosylated proprotein and monitor the *in vitro* folding and appearance of cleavage. To achieve this goal, we first used a previously described variant of AIDA-I without a signal sequence that remains confined in the cytoplasm (36). This mutant was co-expressed with the glycosyltransferase Aah, as glycosylation is important to ensure the normal conformation of the protein (17). At high levels of induction with IPTG, the AIDA-I proprotein forms inclusion bodies (data not shown). The inclusion bodies can be solubilized with 6 M guanidinium hydrochloride, and the uncleaved form of the protein can be purified by affinity chromatography with the help of an N-terminal six-histidine tag. We were, however, unable to refold this protein even when we tried a broad spectrum of buffers and conditions (data not shown). We hypothesized that the presence of the β-barrel is incompatible with correct folding of the entire protein *in vitro*. To solve this problem we used a mutant of the signal sequence-less version of AIDA-I, which we called AIDA-I* and lacks the α-helix and the β-barrel but can still be cleaved (Fig. 1*A*).

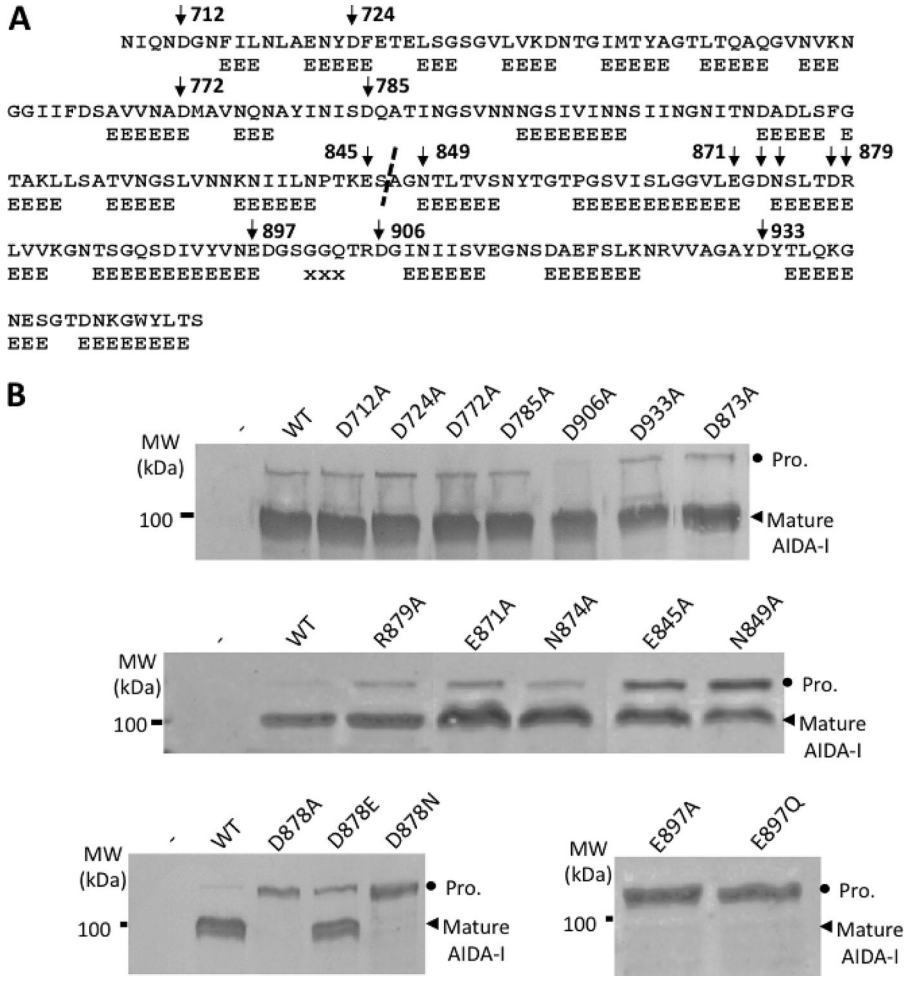

FIGURE 5. **Mutational analysis of the region involved in AIDA-I cleavage.** *A*, predicted secondary structure of the region of AIDA-I encompassing the amino acids between Asn-708 and Ser-953; *E*, β-strand; *x*, no prediction. The positions corresponding to modified amino acids are indicated. The *dashed line* indicates the cleavage site. The numbering of amino acids corresponds to the position in full-length pre-proprotein. *B*, whole-cell lysates were obtained from overnight cultures of C600 harboring an empty vector (−), plasmid pAgH (*WT*), or one of the plasmids bearing a point mutation in pAgH. Proteins separated by SDS-PAGE were probed by immunoblotting with antibodies against the His tag, which allowed the detection of the proprotein (*Pro.*, *circles*) and the mature AIDA-I (*arrowheads*).

The uncleaved AIDA-I* protein was solubilized from inclusion bodies in 6 M guanidinium hydrochloride and purified. Renaturation was performed by exchanging guanidinium hydrochloride with a renaturation buffer. Cysteine and serine protease inhibitors were added to the renaturation buffer to limit the risk of an unspecific cleavage being mediated by contaminating proteases. As shown in Fig. 1*B*, mature AIDA-I* becomes detectable 43 h after buffer exchange and increases in quantity throughout the experiment. Furthermore, the appearance of the mature AIDA-I* is concomitant with a reduction in the amount of proprotein. The time course of mature AIDA-I* appearance could be fitted to a single exponential with a rate constant of 0.53 ± 0.19 min^{-1} (Fig. 1*B*). We used a 16% Tris-Tricine gel to visualize the C-terminal peptide that would result from the cleavage of the proprotein into mature AIDA-I*. As shown in Fig. 1*C*, the 11-kDa fragment appears after renaturation of the protein but is absent from an uncleaved mutant, used as control (see below). This experiment shows that AIDA-I is processed by an autocatalytic event. We noted, however, that this *in vitro* cleavage was less efficient than the fast and complete cleavage that is usually observed in bacteria expressing AIDA-I. Indeed, uncleaved protein remains even after 6 days of renaturation. This could be due to slow and incomplete folding, as shown below.

We used mass spectrometry on *in vitro* refolded mature AIDA-I* to determine the precise location of the cleavage observed. As expected, the same C-terminal peptide as for native AIDA-I, ^{837}NIILNPTKES^{846}, was found, confirming that the cleavage occurs at the usual site during the *in vitro* refolding, between Ser-846 and Ala-847 (19). To exclude the possibility that cleavage resulted from a contaminating protease, we performed refolding experiments with a variant of AIDA-I* bearing a point mutation in one putative catalytic residue (mutant detailed below) and showed that this protein is not cleaved in the same conditions (Fig. 1*C*). Taken together, those results are the first direct proof of an autocatalytic cleavage activity for the AIDA-I autotransporter.

Correlation between Folding and Cleavage—The appearance of mature AIDA-I* is strikingly slow, taking more than 1 day. Protein folding is generally thought to be faster, with folding rates calculated in seconds. However, extremely slow *in vitro* folding was already observed with the native pertactin (40), which possesses the same β-helical structure that is predicted for AIDA-I (39). We then wanted to gain insights in the folding kinetics of AIDA-I to assess if cleavage could correlate with protein folding. Evidence of the *in vitro* folding of AIDA-I* was obtained by monitoring the changes in the far UV CD signal of the protein. As shown in Fig. 1*D*, gain of structure was evident in the CD signal over time after exchange with renaturation buffer, but the appearance of secondary structure was remarkably slow. The time course monitored at 218 nm (Fig. 1*E*) can be fitted to a single exponential with a rate constant of 0.74 ± 0.17 min^{-1}, which is consistent with the kinetics of appearance of mature AIDA-I.

To confirm this observation, we used a common characteristic of folded protein; that is, resistance to proteolysis. At different time points during refolding, a sample was submitted to a 30-min protease treatment. Most of mature AIDA-I* was resistant to the protease at all time points where it was visible, whereas the proprotein was completely susceptible (Fig. 2). Taken together, these results strongly suggest that mature

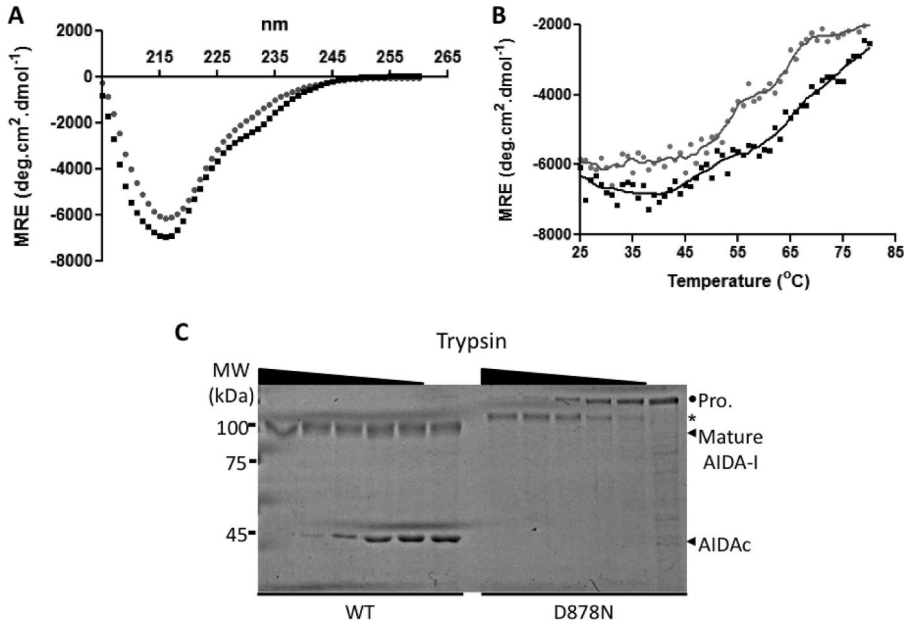

FIGURE 6. **Characterization of the D878N protein.** *A*, far-UV CD spectra of the purified AIDA-I wild-type protein (*gray circles*) and the uncleaved D878N mutant (*black squares*). The ellipticities were recorded between 205 and 260 nm. *B*, the ellipticities at 218 nm of the WT protein (*gray circles*) or the D878N mutant (*black squares*) were recorded with the temperature varying between 25 and 80 °C at a rate of 5 °C/min. *MRE*, mean residual ellipticity. *C*, purified uncleaved (D878N) and cleaved (WT) proteins were incubated in the presence of different concentrations of trypsin. The proteins were resolved by SDS-PAGE, and the gel was stained with Coomassie Blue.

AIDA-I* is indeed folded and that folding and cleavage of AIDA-I* are two closely related events.

*Effect of pH on the in Vitro Refolding of AIDA-I**—The efficiency of AIDA-I* *in vitro* folding was examined at pH 4, 6, and 10. We observed that the refolding buffer used had a marked effect on the refolding kinetics of AIDA-I*. At pH 10, the protein remains unfolded, even 145 h after buffer exchange (Fig. 3*A*). No cleavage was apparent at all time points (Fig. 3*B*), and the protein was completely susceptible to protease digestion (Fig. 3*C*), confirming the absence of renaturation at pH 10. At pH 6 the renaturation of AIDA-I* was close to what we observed at pH 8, with a similar folding rate, cleavage kinetics, and protease resistance (Fig. 3).

At pH 4, the protein appeared to be almost completely folded immediately (Fig. 3*A*). However, it was uncleaved and remained uncleaved even after 6 days (Fig. 3*B*). Because charged residues are involved in the cleavage (see below), we shifted the pH back to pH 8 in the hope to trigger cleavage. Even 145 h after the pH shift, no cleavage was observed (Fig. 3*C* and data not shown). Surprisingly, the protein was partially susceptible to added trypsin, leaving a stable fragment of ~23 kDa (Fig. 3*C*), in sharp contrast with the protein refolded at pH 6 or 8. These results suggest that the renaturation of the AIDA-I* protein at pH 4 is fast but aberrant, an observation that could explain the absence of proteolytic cleavage. Taken together, these results highlight a striking pH dependence of AIDA-I* *in vitro* folding. In addition, these experiments reinforce the observation that cleavage is closely related to the proper folding of the protein and argue that the *in vitro* cleavage we observed is significant and specific.

Mapping of the Region Involved in AIDA-I Cleavage—To support our model of autocatalytic cleavage, we decided to map the region of the protein involved in the cleavage reaction. To address this question, we used different deletion mutants and assessed the capacity of the resulting proteins to process themselves. The AIDAΔN (deletion of amino acids 45–225), AIDAΔC2 (deletion of amino acids 224–667), AIDAΔSS (deletion of the entire signal sequence, amino acids 2–49), and the AIDA-I* mutant were tested for their ability to process themselves (Fig. 4*A*). All mutants were coexpressed with the glycosyltransferase Aah, and whole-cell lysates were probed with antibodies against the His tag. As shown in Fig. 4*B*, all deletion mutants were cleaved, with appearance of mature proteins at the expected sizes. For the AIDAΔC2 protein, two different bands appeared, one at the expected size and another one slightly lower that may correspond to a degradation product. We have previously observed that this mutant is indeed unstable (37). Overall, these results suggest that the AIDA-I catalytic site is located between Ala-667 and Thr-953, a region encompassing the conserved junction domain of autotransporters (amino acids Thr-851 to Leu-952) as well as a part of mature AIDA-I including the cleaved peptidic bond (between Ser-846 and Ala-847).

Two Acidic Residues Are Required for AIDA-I Cleavage—None of the classical sequences for aspartyl, serine, or metalloproteases could be identified in AIDA-I. Furthermore, as this protein lacks cysteine residues, we ruled out the possibility of cysteine protease activity. Other autotransporters of *E. coli* belonging to the SPATE family are autocatalytically cleaved by a novel mechanism involving an asparagine and an aspartate residue embedded in the β-barrel (29). Also, some bacterial aspartate proteases do not possess the classical D(S/T)G consensus motif, as for instance is the case with omptins (41). We, therefore, hypothesized that aspartate residues may be responsible for AIDA-I cleavage.

To test this hypothesis we exchanged several aspartate residues between Ala-667 and Thr-953 with alanines (Fig. 5*A*). This amino acid was chosen because it is less likely to negatively influence the catalytic activity and the folding of the mutated proteins. For all mutants, whole-cell lysates were obtained and probed with antibodies against the His tag. As shown in Fig. 5*B*, most of the mutations did not affect the biogenesis or the cleavage of the protein. For the D878A mutant, however, only the proprotein form was observed, suggesting an inhibition of cleavage. The fact that processing is completely abolished strongly suggests that this aspartate plays a catalytic role. To test the requirement for the carboxyl group of the aspartate in position 878, as would be expected if it were to be catalytic, we changed this amino acid by an asparagine or by a glutamate. Conservation of the carboxyl group maintained the cleavage,

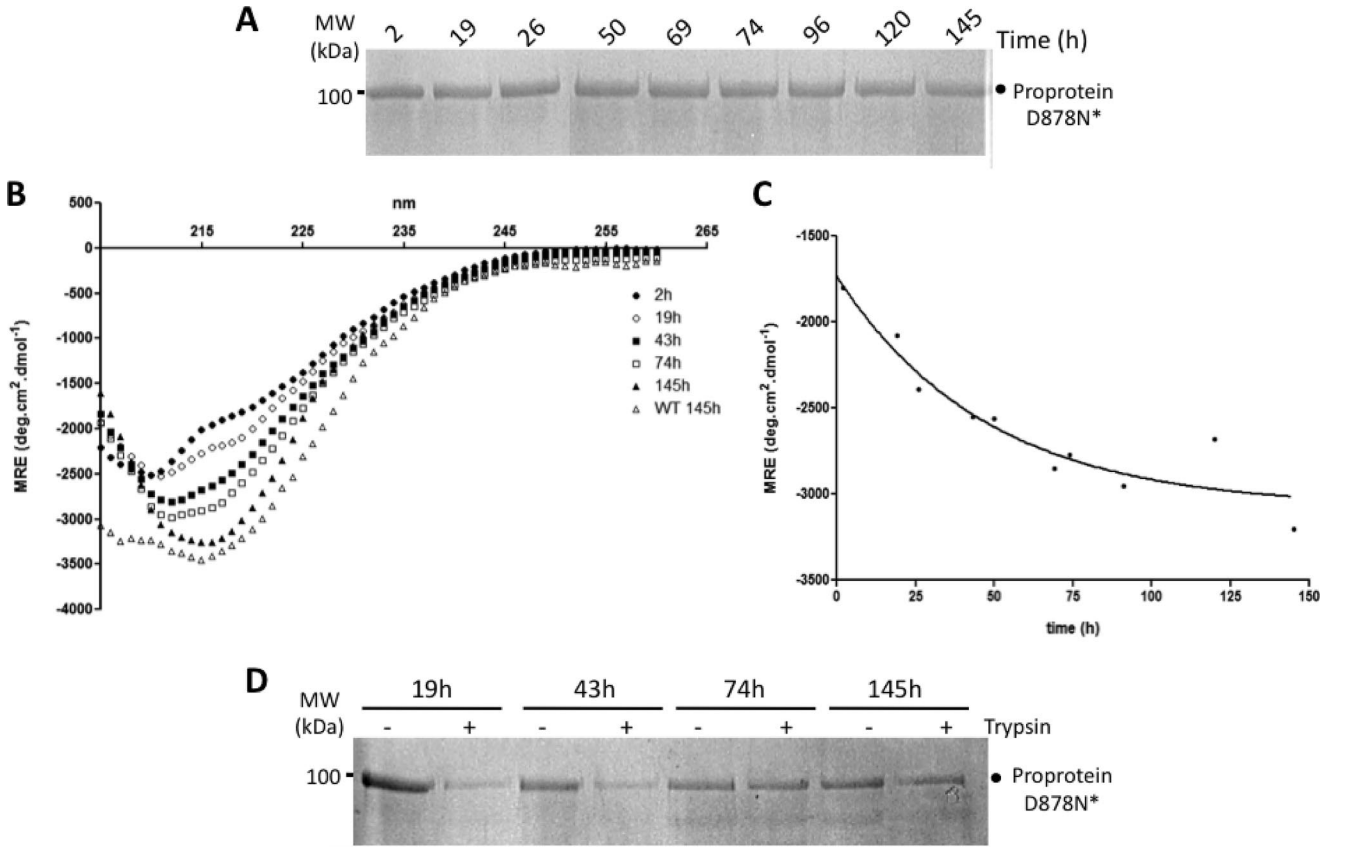

FIGURE 7. **Renaturation and folding kinetics of D878N* mutant.** The D878N* protein was purified as described in Fig. 1. *A*, at different times after buffer exchange, aliquots were taken and boiled in SDS-PAGE loading buffer. The proteins were then resolved by SDS-PAGE, and the gel was stained with Coomassie Blue. The uncleaved (proprotein D878N*, *circles*) form of the protein is indicated. *B*, far-UV CD spectra of the D878N* protein. The ellipticities were recorded between 205 and 260 nm. The CD spectrum of the WT AIDA-I* after 145 h of renaturation is indicated. *C*, the ellipticities at 218 nm were recorded at different times after the initial renaturation. *MRE*, mean residual ellipticity. *D*, limited proteolysis was performed as described in Fig. 2. The proteins were resolved by SDS-PAGE, and the gel was stained with Coomassie Blue.

whereas the modification by an asparagine residue abolished completely the processing of AIDA-I.

As aspartic proteases usually form a catalytic dyad or triad, we decided to change into alanines some of the polar amino acids around Asp-878. We chose Glu-845, Asn-849, Glu-871, Asn-874, Arg-879, and Glu-897. The cleavage was slightly altered in two mutants, E845A and N849A, which are localized near the cleavage site. One mutation, however, E897A, resulted in the complete abolition of processing. The cleavage was still inhibited when the glutamate was changed into glutamine, highlighting a role for this second carboxyl group in the cleavage reaction. We also modified all aspartate residues (Asp-1021, -1078, -1117, -1170, -1175, -1233, -1234) predicted to be located in the extracellular loop of the β-barrel of AIDAc and which, therefore, could potentially be spatially close to the cleavage site, but none of the mutations resulted in a reduction of the processing (data not shown). Taken together, our results suggest that Asp-878 and Glu-897 form a catalytic dyad of carboxylic amino acids, which is common in aspartic proteases.

Characterization of the D878N Uncleaved Mutant—We compared the adhesive, self-aggregation, and biofilm formation activities mediated by the uncleaved D878N mutant and the WT protein. We observed that the D878N mutant is as functional as the wild type in all assays (data not shown). This is consistent with our previous observation obtained with a protein mutated at the cleavage site (15). The diminished AIDA-I cleavage in this mutant did not affect the functionality of the protein.

We purified the WT and the D878N proteins from the outer membrane in their native conformations and compared their secondary structure, stability, and relative protease resistance. The far UV CD spectrum for the D878N mutant is slightly different from the spectrum of the WT protein (Fig. 6*A*). However, by following the thermal denaturation at 218 nm continuously while changing the temperature between 25 °C and 80 °C, we observed that the thermal denaturation of the two proteins is almost identical (Fig. 6*B*). Last, the conformation of the uncleaved mutant was assayed by protease resistance, and as illustrated in Fig. 6*C*, the two proteins showed the same resistance to trypsin, in agreement with the thermal denaturation. We noted that it is only AIDAc that seems to be sensitive to the protease but did not investigate further. Overall, these results show that the uncleaved mutant behaved almost indistinguishably from the wild-type protein.

In Vitro Refolding of the D878N Uncleaved Mutant—We then wanted to compare the *in vitro* refolding kinetics of the D878N mutant with that of the wild-type protein. We introduced the D878N mutation in the plasmid pAngHΔSSΔ$\alpha\beta$, generating the D878N* protein. We purified D878N* from inclusion bodies and performed the *in vitro* renaturation as

described above with the wild-type protein. As shown in Fig. 7*A*, in contrast to the WT protein, the D878N* mutant remained in the uncleaved form, even 145 h after the buffer exchange. The absence of cleavage was confirmed by the lack of the 11-kDa peptide that was present with the wild-type AIDA-I* protein (Fig. 1*C*).

We also monitored the changes in the far UV CD of D878N*. As was the case with the WT protein, the folding of the uncleaved mutant was especially slow (Fig. 7*B*). As observed above with the native proteins, we noted a small difference in the final CD spectrum for the D878N mutant in comparison to the WT protein. Again, this suggests the existence of a subtle difference in secondary structure between the two proteins. The refolding time course monitored at 218 nm could be fitted to a single exponential with a rate constant of 1.09 ± 0.39 min^{-1}, similar to the kinetics of the wild-type protein (Fig. 7*C*). To confirm the renaturation of the D878N mutant, we submitted the protein to a 30-min protease treatment. As shown in Fig. 7*D*, the percentage of protein resistant to protease increased with time, confirming the *in vitro* refolding of this protein. Taken together, these results suggest that the *in vitro* folding kinetics of the AIDA-I* and the D878N* proteins are similar, arguing that *in vitro* cleavage observed with wild-type AIDA-I* is directly linked to the presence of the amino acid Asp-878.

AIDA-I Is Cleaved by an Intramolecular Mechanism—In a previous publication we showed that the cleavage of AIDA-I was independent of its expression level (15). This observation was consistent with an intramolecular processing but proof that this is indeed the case is still missing. We performed the *in vitro* refolding at concentrations of AIDA-I* varying between 150 and 400 $\mu g \cdot ml^{-1}$ to evaluate the effect of protein concentration on the kinetics of cleavage. The appearance of mature AIDA-I* fitted single exponentials with rate constants that were not significantly different (0.77 ± 0.22 min^{-1} at 150 $\mu g \cdot ml^{-1}$, 0.53 ± 0.19 min^{-1} at 200 $\mu g \cdot ml^{-1}$, 0.70 ± 0.26 min^{-1} at 250 $\mu g \cdot ml^{-1}$, and 0.52 ± 0.18 min^{-1} at 400 $\mu g \cdot ml^{-1}$). The independence of cleavage from protein concentration suggests an intramolecular reaction. In addition, we purified the WT and D878N proteins in their native conformation and incubated the two proteins together. As shown in Fig. 8*A*, the level of D878N proprotein remained unchanged even after 2 h of incubation with the WT protein, showing that no intermolecular cleavage could be observed. A similar experiment was performed *in vivo* with bacteria expressing the WT or D878N proteins. After coincubation of the two bacterial cultures for 30 min, no intermolecular cleavage was observed (Fig. 8*B*). Last, we expressed both proteins on the surface of the same bacteria. As shown in Fig. 8*C*, the D878N mutant remained uncleaved in the presence of a functional wild-type protein. Taken together, these results showed that autoproteolysis of AIDA-I is intramolecular.

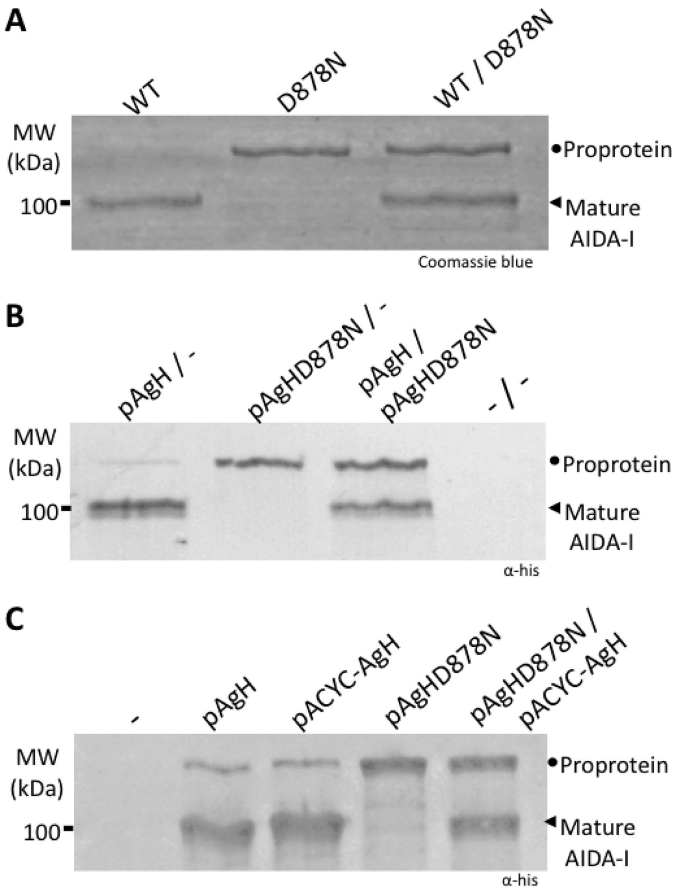

FIGURE 8. **Intramolecular cleavage of AIDA-I.** *A*, wild-type AIDA-I (*WT*) or the uncleaved (*D878N*) proteins were incubated separately or together for 30 min at room temperature and resolved by SDS-PAGE, and the gel was stained with Coomassie Blue. *B*, whole-cell lysates were obtained from overnight cultures of *E. coli* C600 harboring plasmids pTRC99a (−), pAgH (WT), or pAgHD878N (D878N) coincubated for 30 min at 30 °C. The samples were resolved by SDS-PAGE and probed with anti-His tag antibodies, which allowed the detection of the proprotein (*circle*) and the mature AIDA-I (*arrowheads*). *C*, whole-cell lysates from overnight cultures of *E. coli* C600 harboring plasmids pTRC99a and/or PACYC184 (−), pAgH, pACYC-AgH, pAgHD878N, or pACYC-AgH and pAgHD878N were resolved by SDS-PAGE and probed with anti-His tag antibodies.

DISCUSSION

In this study we proved the autocatalytic nature of the cleavage of the AIDA-I autotransporter by following the *in vitro* refolding of a mutant lacking its C-terminal α-helix and β-barrel. We noted that *in vitro* cleavage was less efficient that processing *in vivo*. This could be because of incomplete folding. Indeed, we observed that folding and processing occur at similar rates, which strongly suggests that the two events are closely related. This observation is also evidence against the cleavage, resulting from a contaminant protease, as the folding of AIDA-I is strikingly slow, and an exogenous protease would most likely cleave AIDA-I faster. Furthermore, we observed that the *in vitro* refolding of AIDA-I is dramatically pH-dependent and without folding (pH 10), or with an aberrant folding (pH 4) the protein remains uncleaved, showing more evidence of a strong association between folding and cleavage.

We identified by deletion analysis a 286-amino acid region directly involved in the processing of AIDA-I. This region includes the junction domain, which ends just before the cleavage site and the C-terminal part of the AIDA-I functional domain. We chose to mutate acidic residues of this region because of the observation that *in vitro* refolding and processing of AIDA-I occurred even in the presence of serine and cysteine protease inhibitors. Some acidic proteases, like the omptin family, rely on catalytic aspartate residues that cannot be identified by classical consensus motifs (42). We found that

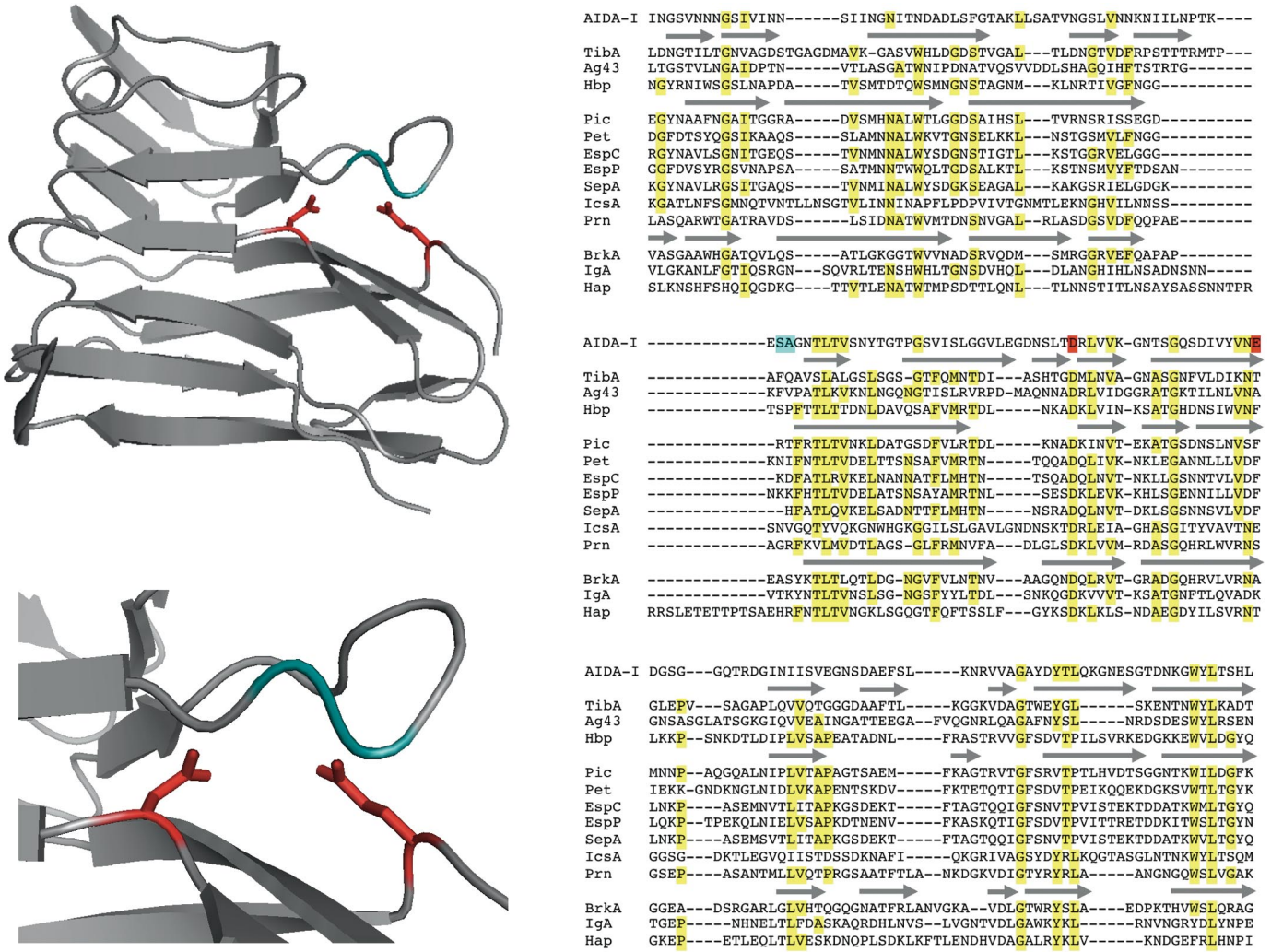

FIGURE 9. **Structural model and alignment of the cleavage site of AIDA-I.** *Left panel*, a three-dimensional structural model of the junction region and the cleavage site of AIDA-I (amino acids Ile-807—Leu-956). The amino acids constituting the cleavage site, Ser-846 and Ala-847, are highlighted in *cyan*, and the amino acids Asp-878 and Glu-897 are highlighted in *red* and depicted with their side chains. The *bottom panel* shows a close-up view of the cleavage site and the Asp-878 and Glu-897 residues using the same color scheme. *Right panel*, alignment of the junction region of several autotransporters. The secondary structure features, either modeled (for AIDA-I) or experimentally determined (for Hbp (48) and Prn (39)), are indicated. The positions of Ser-846, Ala-847, Asp-878, and Glu-897 are highlighted in *cyan* and *red*, as in *A*. The accession numbers for the sequence data and the amino acids range used for the alignment are: ABS20376, amino acids 807–956 (*E. coli* AIDA-I); Q9XD84, amino acids 470–629 (*E. coli* TibA); P39180, amino acids 540–704 (*E. coli* Ag43); O88093, amino acids 919–1073 (*E. coli* Hbp); Q7BS42, amino acids 915–1058 (*E. coli* Pic); O68900, amino acids 836–991 (*E. coli* Pet); AAC44731, amino acids 851–1022 (*E. coli* EspC); Q7BSW5, amino acids 840–996 (*E. coli* EspP); CAA88252, amino acids 911–1062 (*S. flexneri* SepA); CAC05837, amino acids 572–739 (*S. flexneri* IcsA); Q03035, amino acids 416–569 (*B. pertussis* Prn); AAA51646, amino acids 551–706 (*B. pertussis* BrkA); CAA45708, amino acids 828–984 (*H. influenzae* IgA protease); and P45387, amino acids 800–977 (*H. influenzae* Hap).

Asp-878 and Glu-897 in the junction region are involved in the processing of AIDA-I. The complete elimination of cleavage when these residues are mutated strongly suggests that they play a catalytic role. Mutations that preserve the acidic side chain were tolerated, giving more evidence that the carboxylic acid groups are directly involved in catalysis. The requirement of Asp-878 for catalytic activity was confirmed by *in vitro* refolding experiments with the D878N mutant, showing that it can refold but remains uncleaved. We observed that the uncleaved mutant presents a normal global conformation, as this mutant is as functional and as stable as the wild-type AIDA-I. Last, we confirmed that the cleavage of AIDA-I relies on an intramolecular mechanism of processing.

As shown in Fig. 9, our results are consistent with a three-dimensional structural model of the junction region and the AIDA-I cleavage site (the amino acids between Ile-807 and Leu-956), which we generated using the known crystal structure of *B. pertussis* pertactin (39). This model predicts that Asp-878 and Glu-897 are located close to the cleaved peptidic bond, which is found in a loop. This gives an explanation as to why folding and cleavage occur at similar rates; the junction domain of AIDA-I and the region encompassing the cleavage site have to be properly folded for the correct positioning of the catalytic residues in relation to the cleaved peptidic bond. The model also explains why mutations such as E845A or N849A lead to a decrease in the processing efficiency, as these changes would likely destabilize the loop bearing the bond that has to be cleaved.

The mechanism of autocatalytic cleavage we describe here for AIDA-I is unique among the monomeric autotransporter

family. Alignment of the junction region sequences of several autotransporters highlights that Asp-878 of AIDA-I is conserved among autotransporters whether they are processed or not (Fig. 9). However, Glu-897 is unique to AIDA-I among autocatalytic-cleaved autotransporters, which could explain why this mechanism of proteolysis is unique to AIDA-I. Our model also differs from the two previously described intramolecular mechanisms of cleavage for autotransporters; that is, the processing mediated either by endogenous serine protease domains or SPATE and pertactin-like autotransporters.

The cleavage mechanism for several other autotransporters, including the Ag43 aggregation factor, remains unknown. As Ag43 and AIDA-I are closely related in sequence and possess similar functional features (18), it is tempting to hypothesize that a similar mechanism of processing involving carboxylic amino acids exists for Ag43. However, Ag43 is cleaved at a different site compared with the one of AIDA-I (43) and in a region that has only poor homologies with known autotransporter structures.

The question of the function of AIDA-I cleavage remains. In autotransporters that are cleaved the processing can play different roles, such as the release of cytotoxic domains in the extracellular milieu (44), keeping a protein localized at a pole (45), or controlling the expression level of an adhesin (46). The intramolecular nature of AIDA-I processing excludes the possibility that it serves to regulate the protein level at the surface of the bacteria. In addition, we did not observe that cleavage is important for function, as uncleaved mutants resulting from mutations of the catalytic residues or mutations of the residues of the cleaved peptidic bond are as functional as the wild-type protein. This puzzling observation is at least consistent with the fact that we could not find any conditions that lead to the release of mature AIDA-I in the extracellular milieu (15). We can hypothesize that in the context of an animal infection, a specific condition may cause the release of mature AIDA-I, which would be beneficial for the bacteria, for example to escape the immune response. Alternatively, cleavage could generate a new unique surface representing an interaction site with other unknown proteins or host factors, which could play a role during infection. This mechanism was recently observed with the EscU protein, a structural component of the inner membrane ring of the type-three secretion system in *E. coli* (47). This last hypothesis would be consistent with the small differences we observed between CD spectra for the D878N mutant and the WT protein in their native conformations or after *in vitro* folding.

Self-processing of autotransporters is a frequent feature and occurs by a variety of different mechanisms, with our study providing yet another one. This diversity is quite surprising and strongly suggests that this processing plays an important role. Further investigation is, therefore, required to establish what this role might be in the case of AIDA-I.

Acknowledgment—We thank François Lépine for performing the mass spectrometry experiments.

REFERENCES

1. Henderson, I. R., Navarro-Garcia, F., Desvaux, M., Fernandez, R. C., and Ala'Aldeen, D. (2004) *Microbiol. Mol. Biol. Rev.* **68,** 692–744
2. Henderson, I. R., and Nataro, J. P. (2001) *Infect. Immun.* **69,** 1231–1243
3. Girard, V., and Mourez, M. (2006) *Res. Microbiol.* **157,** 407–416
4. Peterson, J. H., Szabady, R. L., and Bernstein, H. D. (2006) *J. Biol. Chem.* **281,** 9038–9048
5. Oomen, C. J., van Ulsen, P., van Gelder, P., Feijen, M., Tommassen, J., and Gros, P. (2004) *EMBO J.* **23,** 1257–1266
6. Barnard, T. J., Dautin, N., Lukacik, P., Bernstein, H. D., and Buchanan, S. K. (2007) *Nat. Struct. Mol. Biol.* **14,** 1214–1220
7. Oliver, D. C., Huang, G., Nodel, E., Pleasance, S., and Fernandez, R. C. (2003) *Mol. Microbiol.* **47,** 1367–1383
8. Renn, J. P., and Clark, P. L. (2008) *Biopolymers* **89,** 420–427
9. Mogensen, J. E., Tapadar, D., Schmidt, M. A., and Otzen, D. E. (2005) *Biochemistry* **44,** 4533–4545
10. Benz, I., and Schmidt, M. A. (1989) *Infect. Immun.* **57,** 1506–1511
11. Niewerth, U., Frey, A., Voss, T., Le Bouguénec, C., Baljer, G., Franke, S., and Schmidt, M. A. (2001) *Clin. Diagn. Lab. Immunol.* **8,** 143–149
12. Chapman, T. A., Wu, X. Y., Barchia, I., Bettelheim, K. A., Driesen, S., Trott, D., Wilson, M., and Chin, J. J. (2006) *Appl. Environ. Microbiol.* **72,** 4782–4795
13. Zhang, W., Zhao, M., Ruesch, L., Omot, A., and Francis, D. (2007) *Vet. Microbiol.* **123,** 145–152
14. Sherlock, O., Schembri, M. A., Reisner, A., and Klemm, P. (2004) *J. Bacteriol.* **186,** 8058–8065
15. Charbonneau, M. E., Berthiaume, F., and Mourez, M. (2006) *J. Bacteriol.* **188,** 8504–8512
16. Benz, I., and Schmidt, M. A. (2001) *Mol. Microbiol.* **40,** 1403–1413
17. Charbonneau, M. E., Girard, V., Nikolakakis, A., Campos, M., Berthiaume, F., Dumas, F., Lépine, F., and Mourez, M. (2007) *J. Bacteriol.* **189,** 8880–8889
18. Klemm, P., Vejborg, R. M., and Sherlock, O. (2006) *Int. J. Med. Microbiol.* **296,** 187–195
19. Suhr, M., Benz, I., and Schmidt, M. A. (1996) *Mol. Microbiol.* **22,** 31–42
20. Benz, I., and Schmidt, M. A. (1992) *Mol. Microbiol.* **6,** 1539–1546
21. Shere, K. D., Sallustio, S., Manessis, A., D'Aversa, T. G., and Goldberg, M. B. (1997) *Mol. Microbiol.* **25,** 451–462
22. van Ulsen, P., van Alphen, L., ten Hove, J., Fransen, F., van der Ley, P., and Tommassen, J. (2003) *Mol. Microbiol.* **50,** 1017–1030
23. van Ulsen, P., Adler, B., Fassler, P., Gilbert, M., van Schilfgaarde, M., van der Ley, P., van Alphen, L., and Tommassen, J. (2006) *Microbes Infect.* **8,** 2088–2097
24. Turner, D. P., Marietou, A. G., Johnston, L., Ho, K. K., Rogers, A. J., Wooldridge, K. G., and Ala'Aldeen, D. A. (2006) *Infect. Immun.* **74,** 2957–2964
25. Fink, D. L., Cope, L. D., Hansen, E. J., and Geme, J. W., 3rd (2001) *J. Biol. Chem.* **276,** 39492–39500
26. Coutte, L., Willery, E., Antoine, R., Drobecq, H., Locht, C., and Jacob-Dubuisson, F. (2003) *Mol. Microbiol.* **49,** 529–539
27. Serruto, D., Adu-Bobie, J., Scarselli, M., Veggi, D., Pizza, M., Rappuoli, R., and Aricò, B. (2003) *Mol. Microbiol.* **48,** 323–334
28. Pohlner, J., Halter, R., Beyreuther, K., and Meyer, T. F. (1987) *Nature* **325,** 458–462
29. Dautin, N., Barnard, T. J., Anderson, D. E., and Bernstein, H. D. (2007) *EMBO. J.* **26,** 1942–1952
30. Henderson, I. R., and Owen, P. (1999) *J. Bacteriol.* **181,** 2132–2141
31. Nguyen, V. Q., Caprioli, R. M., and Cover, T. L. (2001) *Infect. Immun.* **69,** 543–546
32. Vandahl, B. B., Pedersen, A. S., Gevaert, K., Holm, A., Vandekerckhove, J., Christiansen, G., and Birkelund, S. (2002) *BMC Microbiol.* **2,** 36
33. Ohnishi, Y., Beppu, T., and Horinouchi, S. (1997) *J. Biochem.* **121,** 902–913
34. Litwin, C. M., and Johnson, J. M. (2005) *Infect. Immun.* **73,** 4205–4213
35. Litwin, C. M., Rawlins, M. L., and Swenson, E. M. (2007) *Infect. Immun.* **75,** 5255–5263
36. Charbonneau, M. E., and Mourez, M. (2008) *Res. Microbiol.* **159,** 537–544
37. Charbonneau, M. E., and Mourez, M. (2007) *J. Bacteriol.* **189,** 9020–9029

38. Bennett-Lovsey, R. M., Herbert, A. D., Sternberg, M. J., and Kelley, L. A. (2008) *Proteins* **70,** 611–625
39. Emsley, P., Charles, I. G., Fairweather, N. F., and Isaacs, N. W. (1996) *Nature* **381,** 90–92
40. Junker, M., Schuster, C. C., McDonnell, A. V., Sorg, K. A., Finn, M. C., Berger, B., and Clark, P. L. (2006) *Proc. Natl. Acad. Sci. U. S. A.* **103,** 4918–4923
41. Vandeputte-Rutten, L., Kramer, R. A., Kroon, J., Dekker, N., Egmond, M. R., and Gros, P. (2001) *EMBO J.* **20,** 5033–5039
42. Hritonenko, V., and Stathopoulos, C. (2007) *Mol. Memb. Biol.* **24,** 395–406
43. Klemm, P., Hjerrild, L., Gjermansen, M., and Schembri, M. A. (2004) *Mol. Microbiol.* **51,** 283–296
44. Navarro-García, F., Canizalez-Roman, A., Luna, J., Sears, C., and Nataro, J. P. (2001) *Infect. Immun.* **69,** 1053–1060
45. d'Hauteville, H., Dufourcq Lagelouse, R., Nato, F., and Sansonetti, P. J. (1996) *Infect. Immun.* **64,** 511–517
46. Fink, D. L., and St. Geme, J. W., 3rd (2003) *J. Bacteriol.* **185,** 1608–1615
47. Zarivach, R., Deng, W., Vuckovic, M., Felise, H. B., Nguyen, H. V., Miller, S. I., Finlay, B. B., and Strynadka, N. C. (2008) *Nature* **453,** 124–127
48. Otto, B. R., Sijbrandi, R., Luirink, J., Oudega, B., Heddle, J. G., Mizutani, K., Park, S. Y., and Tame, J. R. (2005) *J. Biol. Chem.* **280,** 17339–17345